INTERNATIONAL JOURNAL OF INTEGRATED ENGINEERING
ISSN: 2229-838X e-ISSN: 2600-7916

IJIE

Vol. 17 No. 1 (2025) 176-189
https://publisher.uthm.edu.my/ojs/index.php/ijie

Investigation on the Optimum Cement–Slag Artificial Aggregates at Different CO_2 Curing Regime

Abila Hena Anayet[1], Nur Hafizah A. Khalid[1]*, Nurdalina Syuhada Zulkifli[1], Siti Aishah Jupri[1], Md Sajid Alam[1], Mohamad Haqzim Ayob[1], Nor Hafizah Berahim[2], Hazratul Mumtaz Lahuri[2], Farahdila Kadirkhan[2]

[1] *Department of Structure and Materials, Faculty of Civil Engineering, Universiti Teknologi Malaysia, 81310 Johor Bahru, Johor, MALAYSIA*
[2] *PETRONAS Research Sdn. Bhd., 43000 Kajang, Selangor, MALAYSIA*

*Corresponding Author: nur_hafizah@utm.my
DOI: https://doi.org/10.30880/ijie.2025.17.01.015

Article Info

Received: 21 August 2024
Accepted: 15 December 2024
Available online: 30 April 2025

Keywords

Artificial aggregates, cement–slag artificial aggregates, CO_2 curing, CO_2-air curing, CO_2-water curing, CO_2 capturing mechanism

Abstract

Carbon dioxide (CO_2) capturing is an attractive approach for producing low carbon construction materials such as artificial aggregates. Therefore, this paper investigates the optimization of cement–slag artificial aggregates under different CO_2 curing regimes. The mix proportion used is 50% Ground Granulated Blast Furnace Slag (GGBS) and 50% Ordinary Portland Cement (OPC) with 20% of water under various curing conditions. The curing regimes include CO_2 curing followed by water and air curing at different curing ages: 1 day of CO_2 curing followed by 27 days of water and air curing, 2 days of CO_2 curing followed by 26 days of water and air curing, and 3 days of CO_2 curing water 25 days of water and air curing; with 28 days of total curing, respectively. After through curing process, several tests were carried out on cement–slag artificial aggregates including an individual strength test, aggregate crushing value test, visual carbonation by phenolphthalein solution and CO_2 uptake by thermogravimetric analysis test. These tests provide a thorough assessment of the artificial aggregates by examining their strength and chemical characteristics under various curing conditions. The results indicated that 3 days of CO_2 curing followed by 25 days of air curing is optimal, showing 6.71 MPa of individual crushing strength and 18.56% of aggregate crushing value. Thermogravimetric analysis indicated that calcium hydroxide ($Ca(OH)_2$) played a significant role in synthesizing calcium silicate hydrate (C–S–H) gel, contributing to aggregate strength. The carbonation of $Ca(OH)_2$ to calcium carbonate ($CaCO_3$) enhanced aggregate durability by reducing permeability and increasing material density. The findings show that the optimal curing regime produces the best results in terms of strength and CO_2-capturing properties, which was the main goal of this study.

1. Introduction

As humanity strives for progress, the challenge of global warming especially in construction industry has become increasingly apparent. The production of cement and concrete contributed to approximately 7% of global

greenhouse gas emissions [1]. Moreover, the depletion of natural aggregate resources highlights the urgent need for alternative materials with equivalent properties to meet construction demands [2].

With the aim of reducing CO_2 emissions, CO_2 will be incorporated into the curing regime, utilizing CO_2 curing as one of the established techniques. During the process, the reaction between CO_2 with cement clinker such as tricalcium silicate (C_3S), dicalcium silicate (C_2S), calcium silicate hydrate (C-S-H) and calcium hydroxide ($Ca(OH)_2$) formed calcium carbonate [3], [4]. The formation $CaCO_3$ fills the pore which subsequently improve the strength of the concrete [5]. Another method to reduce CO_2 emission is by incorporating alkaline-rich industrial waste such as fly ash, ground granulated blast slag (GGBS) and steel slag into the production of artificial aggregates through mineral carbonation. In this process, the alkaline-rich materials inside the artificial aggregate react with CO_2 to form stable carbonate such as $CaCO_3$ and magnesium carbonate ($MgCO_3$) [6]. Among the alkaline-rich industrial waste, selection of GGBS is gaining interest as it is reported to have excellent micro-aggregate effect, good strength and durability as a result of its rich calcium concentration [7]. This approach not only conserves resources but also addresses environmental challenges [8]. The production of artificial aggregates made from slag contributes both to the reduction of CO_2 emissions and the efficient repurposing of industrial byproducts.

In cementitious materials, the hydration process is important to obtain high strength concrete. The exploration of optimized curing regime is necessary as it directly influences the performance of the concrete [9]. Curing concrete in water provides a conducive environment for hydration and protection from rapid moisture loss [10]. Meanwhile, air curing utilizes atmospheric moisture to hydrate the subject. Air curing is generally employed in conjunction with other curing method as to provide sufficient time for the concrete to improve its strength. Several studies have shown that employing various curing techniques such as air, water and CO_2 curing can affect the mechanical and physical properties of these aggregates. It is reported that CO_2 curing has shown encouraging results in terms of durability and compressive strength of cement cylindrical samples as compared to water curing [11], [12]. Another study regarding curing regime revealed that the cement paste which has gone through CO_2 curing followed by water curing experience delayed hydration which is reflected in its microstructural properties [13]. Meanwhile, Liu reported that the artificial aggregates which are subjected to CO_2 and air curing exhibited improved compactness due to formation of $CaCO_3$ [14]. Although artificial aggregates have the potential to improve sustainability, their wider implementation is hindered by the uncertainty around the best curing schedules [15].

Beyond environmental benefits, carbonated artificial aggregates require a deeper understanding of their impact on steel reinforcement corrosion in concrete structures. The carbonation process, while effective at reducing porosity and improving the mechanical properties of concrete, can have significant implications for the durability of steel reinforcements [16]. Carbonation lowers the pH of the surrounding concrete, potentially leading to the de-passivation of the steel surface and accelerating corrosion in the presence of moisture and oxygen. However, it is reported that the reduction of pH level may not sufficiently initiate the corrosion of reinforcement steel [17], [18]. On the other hand, the effect of accelerated carbonation which can be examined through the visual carbonation observation may require further study as it plays a critical role in determining long-term durability and structural integrity [17]. To assess the long–term performance of these aggregates in building applications and to improve the CO_2 curing procedure, more study is necessary.

The point load test is used to assess the individual crushing strength of the artificial aggregate. Meanwhile, the aggregate crushing value (ACV) test evaluates their mechanical strength and durability, particularly for recycled concrete aggregates (RCA) [12], [18], [19]. Besides, thermogravimetric analysis and derivative thermogravimetric (TGA/DTG) curve provides insight into the reaction rates and thermal properties of a material which is crucial to understand the CO_2 capturing mechanism of artificial aggregates.

In summary, this study aims to identify the optimum curing regimes for carbonated artificial aggregates made from cement and GGBS by comparing their mechanical and CO_2-capturing properties. The mechanical properties of the cement-slag artificial aggregates will be determined through individual crushing strength test and aggregate crushing value (ACV) while the CO_2-capturing properties will be verified by visual carbonation test using phenolphthalein solution as well as TGA/DTG curve analysis. Through detailed investigation and analysis, this work seeks to offer insights into the use of carbonated aggregates to enhance both material performance and environmental sustainability.

2. Experimental Procedure

2.1 Preparation of Cement–Slag Artificial Aggregates

The granulation process was a crucial stage in the production of cement–slag artificial aggregates that were made from a blend of Ordinary Portland Cement (OPC) and Ground Granulated Blast Furnace Slag (GGBS). To modify the cement–slag artificial aggregates properties like strength, durability, and workability, the ideal ratio between OPC and GGBS needed to be calculated. The precise blend of 50% of OPC and 50% of GGBS was calculated to optimize their synergistic interaction, resulting in a well–balanced mixture. To create this the cement–slag

Int. Journal of Integrated Engineering Vol. 17 No. 1 (2025) p. 176-189

artificial aggregates with optimal workability and strength for concrete applications, 3 kg of aggregates were prepared using a 50:50 ratio of OPC (1.5 kg) and GGBS (1.5 kg). The chemical compositions of OPC and GGBS were determined using energy-dispersive x-ray fluorescence (EDXRF) spectroscopy (see Table 1).

Table 1 *Chemical composition of OPC and GGBS (wt. %)*

Chemical properties	Percentage (%)	
	OPC	GGBS
SiO_2	14.60	29.73
CaO	60.00	37.84
Fe_2O_3	2.20	1.37
Al_2O_3	3.34	15.55
MgO	0.62	6.60
SO_3	2.63	0.86
MnO	-	0.51
TiO_2	0.21	-
P_2O_5	-	0.01

Initially, the granules were formed by mixing the OPC and GGBS (see Fig. 1(a)), followed by spraying water. The resulting granules were referred to as cement–slag artificial aggregates (see Fig. 1(b)). To ensure optimal binding in the formation of the artificial aggregates, the water content was measured at approximately 20% of the total mixture. The granulator was set to an angle of 30° with an operating speed of 35 rpm for a 30-minute formation process, which helped achieve uniform cement–slag artificial aggregates. The artificial aggregates were then exposed to direct CO_2 gas at 98% purity, with a flow rate of 5 L/min at 1 bar pressure for approximately 30 minutes. Next, the artificial aggregates were sieved to get a proper and consistent particle size distribution. Fig. 2 illustrates the particle distribution of artificial aggregates that provide important information on the materials' gradation, which could help in terms of the hydration of cement and the strength of the concrete.

(a) **(b)**

Fig. 1 *Disc granulator (a) Mix of OPC and GGBS; (b) Formation of cement–slag artificial aggregates*

Fig. 2 *Particle size distribution of cement–slag artificial aggregates*

2.2 Curing Regimes

2.2.1 CO_2 Curing

The cement–slag artificial aggregates were then cured in CO_2 chamber, where pure CO_2 gas was injected into the chamber at 1 bar with a concentration of 19.9% ± 0.1% and a fixed temperature of 59.9°C ± 0.1 °C to accelerate the CO_2 curing process for 1, 2 and 3 days, followed by further curing under different regimes with the designed notation: (a) CO_2–water curing, which involved CO_2 curing followed by water curing; and (b) CO_2–air curing, which involved CO_2 curing followed by air curing. The purpose of extending the curing process after CO_2 curing under different regimes was to reduce energy consumption during CO_2 curing and to ensure continuous curing until a minimum total curing age of 28 days for artificial aggregates. The curing process played a pivotal role in the production of artificial aggregates, aiding in terms of their strength development, durability, and attainment of desired properties. Fig. 3(a) illustrates the CO_2 chamber that was used in this study.

2.2.2 CO_2–Water Curing

The cement–slag artificial aggregates were further cured with tap water after 1, 2 and 3 days of CO_2 curing process. They were carefully transferred and immersed in water for a duration of 25, 26, and 27 days, respectively, to achieve a minimum total curing age of 28 days. Fig. 3(b) illustrates the artificial aggregates under the water-curing process. This immersion enables the cementitious matrix within the artificial aggregates to continue hydrating and developing. Each immersion phase marks a critical stage in the curing process, facilitating the enhancement and strengthening of the aggregates' mechanical properties.

2.2.3 CO_2–Air Curing

The cement–slag artificial aggregates were further subjected to air curing after 1, 2 and 3 days of the CO_2 curing process. The artificial aggregates were left in the room with an ambient air environment for predetermined periods of 25, 26 and 27 days, respectively, to fulfill the minimum total curing age requirement of 28 days. Fig. 3(c) displays the artificial aggregates exposed to air curing after the CO_2 curing process.

Int. Journal of Integrated Engineering Vol. 17 No. 1 (2025) p. 176-189

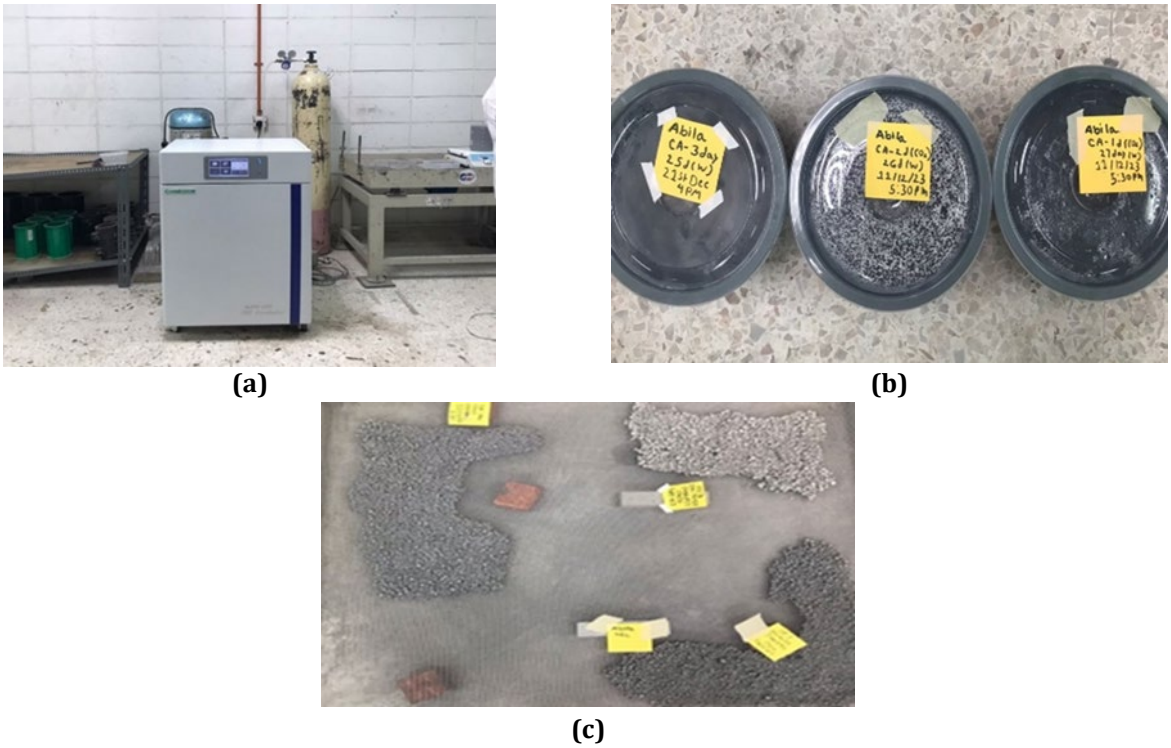

(a) **(b)**

(c)

Fig. 3 *The cement–slag artificial aggregates at different curing regimes (a) CO_2 chamber; (b) Water curing; (c) Air curing*

2.3 Strength Properties

2.3.1 Individual Point Load Test

Although cement–slag artificial aggregates generally exhibit more uniform qualities compared to natural aggregates, the aggregates possess a unique strength, influenced by their production methods. In contrast, natural aggregates may vary in strength due to geological factors. Individual point load tests on artificial aggregates aim to ensure uniformity and reliability. Therefore, this study conducted the individual strength measurements of artificial aggregates through point load testing to understand their consistent and predictable strength, potential characteristics and material source versatility. The individual point load test was conducted according to the ASTM D5731; a method to determine the point load strength index of rock and its application to rock strength classifications.

Initially, the cement–slag artificial aggregates samples were thoroughly cleaned to remove any impurities. Next, an individual granule of artificial aggregates was positioned between the conical platens of the point load machine's setup. Gradual axial loading was applied until the specimen failed, with approximately 20 granules of each mixture tested under this procedure. The load at which each granule of artificial aggregates failed was recorded. Fig. 4(a) illustrates the point load test apparatus utilized in this experiment. Individual strength can be calculated using the following formula:

$$\sigma = \frac{2.8F}{\pi D^2} \tag{1}$$

where σ is the individual crushing strength of artificial aggregates (in MPa), F is the failure load on artificial aggregates (in N) and D is the diameter of artificial aggregates (in mm).

2.3.2 Aggregate Crushing Value (ACV) Test

The aggregate crushing value (ACV) test was performed according to BS 812: Part 110:1990; a recognized method to measure the strength and durability of aggregates. Fig. 4(b) illustrates the apparatus employed for conducting the ACV test for cement-slag artificial aggregates. The test was performed with artificial aggregates passing a 12.5 mm sieve of size and retained on a 10 mm sieve of size. The artificial aggregates were filled into the cylindrical

mould by measuring in three layers of equal depth, whereby each layer was tampered 25 times using a tamping rod.

The universal testing machine was set up by applying compression load to the cylindrical mould filled with the artificial aggregates with a total load of 400 kN for 10 minutes. The load was released and the whole of the sample was removed from the cylinder mould and sieved with 2.36 mm of sieve size to separate crushed and uncrushed artificial aggregate. The percentage of artificial aggregates passed through the sieve was weighed after the test. The ACV was determined using the following formula, which quantifies the ratio of the weighted original sample to the maximum load applied during testing:

$$ACV = \frac{W_A}{W_B} \times 100 \quad (2)$$

where W_A is the weight of fraction passing through the 2.3 mm sieve (in g) and W_B is the weight of the oven–dried samples (in g).

(a) **(b)**

Fig. 4 *Aggregates test (a) Point load test; and (b) ACV test*

2.4 CO_2 Capturing Properties

2.4.1 Visual Carbonation Test by Phenolphthalein Solution

The rapid carbonation test was performed by visually observing the colour changes on the cement–slag artificial aggregates after spraying with phenolphthalein solution following ASTM E70 standard. The visual observation of carbonation of cement-slag artificial aggregates was conducted at 28 days of CO_2–air-cured and CO_2-water cured, and the colour changes clearly can be seen in Fig. 5. The samples must be free from any debris before spraying the phenolphthalein solution and the colour changes on the cement–slag artificial aggregates were observed. The information collected can be used to understand the CO_2 capturing mechanism of artificial aggregates.

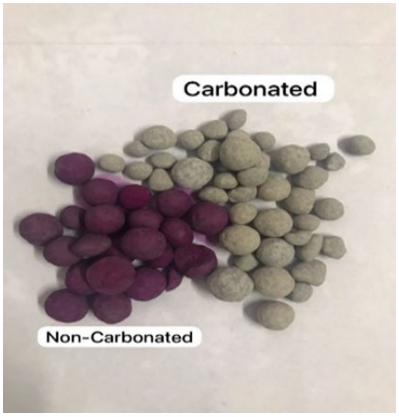

Fig. 5 *Visual observation after spraying with phenolphthalein*

2.4.2 CO_2 Capturing Evaluation by Thermogravimetric Analysis (TGA)

The thermogravimetric analysis (TGA) test was conducted to evaluate the CO_2-capturing properties of cement–slag artificial aggregates. Initially, the aggregates were immersed in acetone solution for 24 hours purposely to stop the cement hydration process. Subsequently, the samples underwent a 24–hour drying process in an oven to eliminate moisture. Then, the samples were crushed and ground into a powder form using a pestle and mortar. The resulting dried powder samples were then subjected to further testing using Thermogravimetric Analyzer Q500 TGA/FT-IR Interface. The dried powder samples were placed into crucibles and subjected to progressive calcination, starting at a temperature of 20°C and gradually increasing to a maximum set temperature of 1000°C, with a temperature ramp rate of 10°C/min. Throughout the testing process, the weights of the samples before and after testing were recorded.

3. Results and Discussion

3.1 Individual Crushing Strength

Fig. 6 shows the effect of CO_2-air curing on the individual strength of three different range sizes of aggregates: 5–6 mm, 7–8 mm and 9–10 mm. The benefits of smaller–sized aggregates are highlighted by the improved strength observed with the 5–6 mm diameter aggregates. The application of smaller particles in the concrete mix is to have a dense packing structure. Due to their compact size, they interlock more tightly and reduce the gaps between the aggregates and matrix [20]. Sharma et al. [21] suggested that using smaller-size aggregates could increase the denseness of the packing structure of the concrete which is essential for minimizing voids. Therefore, the 5–6 mm diameter of artificial aggregates benefited in this study. The smaller particles result in fewer voids and a more homogeneous force distribution across the aggregates, contributing to the overall strength of the concrete application.

Fig. 7 illustrates the effect of water curing on the individual strength of the same sizes of aggregates ranging from 5–6 mm, 7–8 mm and 9–10 mm. Water curing significantly enhances the properties of the concrete mix by maintaining moisture levels which is crucial for the hydration process of the cement. The 5–6 mm diameter aggregates show an improvement in strength in water curing conditions. The application of smaller aggregates can facilitate better interaction in the concrete mix, thus promoting superior adherence and coating by the cement. These results show a strong bond that can enhance cohesiveness and improve the overall compressive strength of the concrete. For the sizes 7–8 mm and 9–10 mm of aggregates, water curing still offers benefits, but the impact is less pronounced compared to the 5–6 mm aggregates. Studies conducted by Yu et al. [22] have shown that larger aggregate sizes while providing structural support, do not achieve the same level of compactness and particle interlocking as smaller ones. However, the water-curing process aids in reducing stress concentrations and potential weak points within the aggregate's matrix, contributing to a more durable concrete mix.

The phenomenon of achieving the highest strength, particularly when using 5–6 mm diameter aggregates, can be attributed to the combined effects of CO_2 curing for 3 days and air curing for 25 days. These curing conditions significantly influence the short– and long–term strength development of concrete. The initial three days of CO_2 curing likely accelerate the early–age strength development of the aggregates. CO_2 curing promotes the formation of $CaCO_3$ within the aggregates matrix through a process known as carbonation, resulting in a quicker initial strength gain compared to conventional curing methods [23]. Following the initial CO_2 curing phase, the subsequent 25 days of air curing allow the hydration and carbonation process to continue. During air curing, the aggregates are maintained in a controlled environment with optimal humidity and temperature, facilitating ongoing chemical reactions that contribute to the material's strength development. This prolonged curing period enhances the long–term strength and durability of the aggregates [24].

The combined strategy of 3 days CO_2 curing followed by 25 days of air curing, especially for 5–6 mm diameter aggregates, maximizes concrete strength by leveraging both early–age and long–term curing conditions. This approach is further improved by the selection of smaller aggregate sizes, which enhance the concrete mix's cohesiveness and compactness. The findings highlight the critical role of careful aggregate selection and curing techniques in achieving optimal concrete performance.

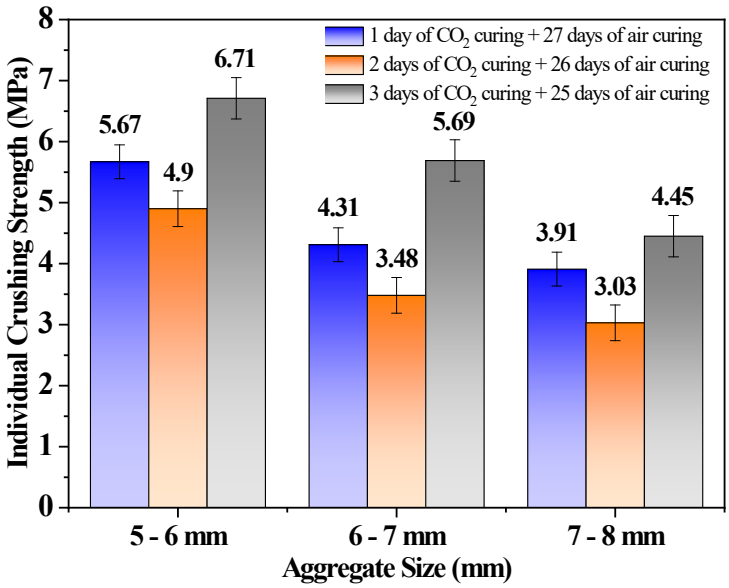

Fig. 6 *Effect of air curing on the individual strength of aggregates of different diameters*

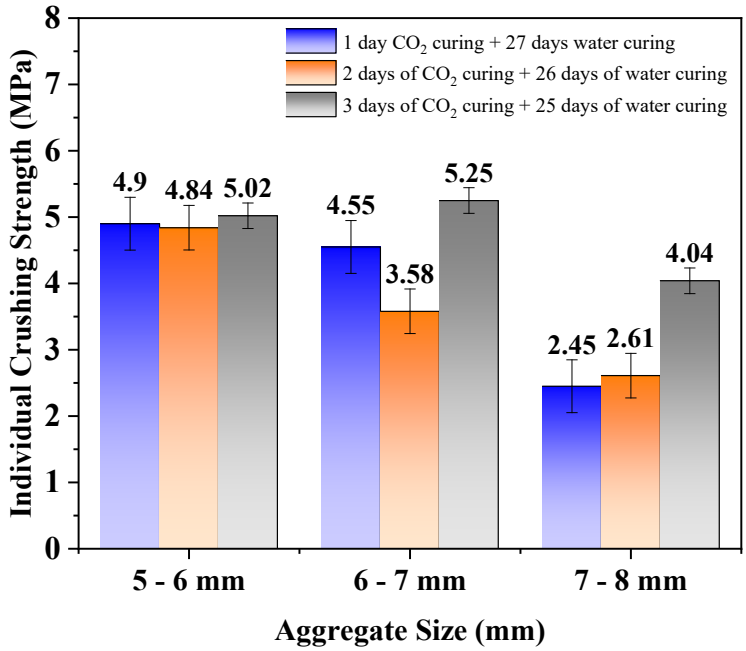

Fig. 7 *Effect of water curing on the individual strength of aggregates of different diameters*

3.2 Aggregate Crushing Value (ACV)

Fig. 8 shows the aggregate crushing value (ACV) under four different conditions. The first exposure to carbonation was critical in the 1 day of CO_2 curing followed by 27 days of air curing conditions when the ACV of 23.32% was seen. $CaCO_3$ was formed inside the aggregate's matrix because of the reaction between CO_2 and $Ca(OH)_2$ from the cement hydration process as follows:

$$Ca(OH)_2 + CO_2 \rightarrow CaCO_3 + H_2O \quad (3)$$

This method helped to increase mechanical strength through void filling and increased interparticle bonding. The air–curing period of 27 days that follows permits continuous hydration and the formation of a tightly bonded aggregate structure. In contrast, the ACV of cement-slag artificial aggregate cured in water was slightly higher (25.22% and 19.0% for initially 1 and 3 days of CO_2 curing, respectively) compared to air curing due to the concentration of dissolved CO_2 gas in the water lower compared to the concentration of CO_2 in the air. A high 19%

Int. Journal of Integrated Engineering Vol. 17 No. 1 (2025) p. 176-189

ACV value of the artificial aggregate which was seen in the 3 days of CO_2 curing followed by 25 days of water curing indicating a slight impact of water on the artificial aggregate properties. This finding highlighted that an excessive amount of water might change the water–to–cement ratio overall, impacting the hydration process. A high–water concentration may cause interparticle bonding to deteriorate, making the aggregates less resistant to crushing.

It is reported that the curing environment affects the aggregate's mechanical characteristics, and how exposure to water may reduce the aggregate's ability to withstand crushing [20]. Nevertheless, the ACV for the 3 days of CO_2 curing followed by 25 days of air curing was quite like the ideal air–cured situation (18.56%). Extended exposure to air promoted sustained hydration and carbonation, which resulted in the formation of an aggregate structure with a strong link. In this case, CO_2-air curing seemed to have a beneficial effect on the crushing resistance of the artificial aggregates. The 3 days of CO_2 curing followed by 25 days of air curing condition was the most advantageous of the examined scenarios. This was proven by the lowest ACV of 18.56%, which indicated higher crushing resistance. A well–balanced mix of air curing and carbonation is responsible for this outcome.

Pang et al. [24] suggested that the aggregate matrix formed $CaCO_3$ because of processes triggered by exposure to CO_2, which improved the mechanical strength by effectively filling voids and forming interparticle bonds. The total curing period of 28 days was essential for continuous hydration, which aids in the formation of a sturdy and tightly bonded aggregate structure. As per previous studies [5], a curing time of 28 days is necessary for the best possible growth of strength.

In addition, previous studies by Ibrahim et al. [25] show that the 3 days of CO_2 curing followed by 25 days of air curing conditions guaranteed ideal moisture management, avoiding an excessive amount of water that might weaken crushing resistance. The well–planned fusion of interparticle bonding, prolonged air curing, carbonation–induced strengthening, and efficient void filling results in a well–bonded aggregate structure that enhances load–bearing capacity and resistance to crushing pressures. This condition stands out as the finest overall due to its all-encompassing approach and optimization of several aspects that affect the aggregate's mechanical strength. The significance of a precisely customized curing approach in achieving the best aggregate performance for building applications was shown by these results. In summary, it can be stated that complex interactions including carbonation effects, air curing advantages, water exposure implications, hydration kinetics, and moisture content dynamics all have an impact on the subtle differences in ACV under various curing circumstances. The results emphasize the necessity of carefully choosing curing methods to maximize aggregate mechanical strength for building applications.

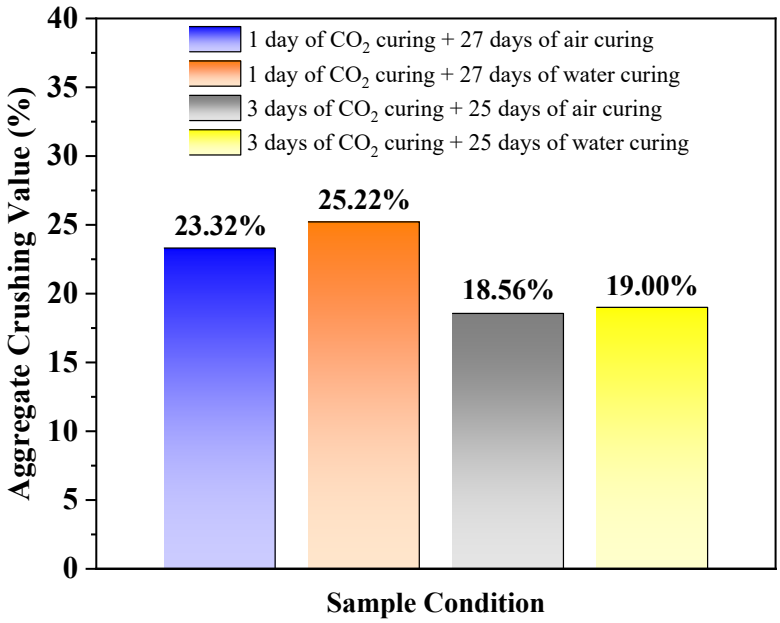

Fig. 8 *ACV under four different sample conditions*

3.3 Visual Carbonation by Phenolphthalein Solution

Fig. 9 shows the visual observation of carbonation after spraying phenolphthalein solution on cement-slag artificial aggregates after 28 days of CO_2–air curing and CO_2-water curing; the colour difference was observed between both curing regimes. For the cement–slag artificial aggregates subjected to CO_2–water curing, the colour immediately turns to pink colour after spraying phenolphthalein solution indicating minimal carbonation. Jiang et al. [26] stated that the samples with this phenomenon retained their alkaline environment due to the lower extent of carbonation. The continuous sample in water curing likely did not facilitate the adsorption of CO_2 which

maintains the pH of alkaline. In contrast, the cement–slag artificial aggregates subjected to CO_2–air curing did not change colour after spraying the phenolphthalein solution, indicating the sample achieved full carbonation. This phenomenon is due to the reaction of $Ca(OH)_2$ from cement with CO_2 which forms stable $CaCO_3$. Additionally, the calcium content in GGBS also reacts with CO_2 which contributes to the formation of $CaCO_3$ [24], [25]. This difference in colour changes was due to the varied curing conditions which CO_2 curing followed by air curing promoting more extensive carbonation.

(a) **(b)**

Fig. 9 *Phenolphthalein indication on cement-slag artificial aggregates at different curing regimes (a) CO_2-water curing (b) CO_2–air curing*

3.4 Thermogravimetric Analysis (TGA)

Among various curing regimes, the artificial aggregate that exhibited the optimum mechanical properties was selected for TGA/DTG analysis. Fig. 10(a) shows the TGA and DTG indicating $Ca(OH)_2$ and $CaCO_3$ decomposition of aggregate samples with 1 day of CO_2 curing followed by 27 days of air curing. Meanwhile, Fig. 10 (b) shows the TGA and DTG curve indicating $Ca(OH)_2$ and $CaCO_3$ decomposition of aggregate samples with 3 days of CO_2 curing followed by 25 days of air curing.

For Fig. 10(a), the weight loss of 2.35% at the temperature ranging from 463.0 °C to 614.8 °C is attributed to the removal of both physically and chemically bound water [26]–[28]. According to Chu et al., these crystals are primarily in the form of $Ca(OH)_2$ [29]. The absence of additional weight loss indicates that the sample is free from organic additives or impurities. The primary cementitious components, such as OPC and GGBS, decompose at various temperatures, contributing to weight loss. Although some cementitious materials contain carbonates, whose decomposition results in weight loss, the extent observed in TGA is not directly proportional to the degree of hydration or the quality of the hydration products formed during the curing process. Nonetheless, the weight loss of 8.58% at a temperature ranging from 614.8°C to 759.8°C indicated the decomposition of $CaCO_3$. The weight percentage of $CaCO_3$ in the aggregate sample can be estimated using the following equation [26]:

$$CaCO_3\ (\%) = \frac{m_{CO2}}{m_{total}} \times \frac{M_{CaCO3}}{M_{CO2}} \times 100\% \quad (4)$$

where m_{CO2} is the product of percentage weight loss due to the decomposition of $CaCO_3$ with the total mass of the sample (in mg), m_{total} is the total mass of the sample (in mg), M_{CaCO3} is the molar mass of $CaCO_3$ (100.09 g/mol) and M_{CO2} is the molar mass of CO_2 (44.01 g/mol).

This calculation is based on the principle that upon the decomposition of $CaCO_3$, CaO remains as a solid residue due to its high decomposition temperature, while CO_2 is released which contributed to the significant weight loss. From Eqn. 4, the weight percentage of $CaCO_3$ in the aggregate sample is calculated to be 19.51%.

Conversely, the aggregates that underwent 3 days of CO_2 curing followed by 25 days of air curing (as shown in Fig. 10(b)) experienced a 2.53% weight loss between 450.6°C and 618.9°C due to the decomposition of $Ca(OH)_2$. The decomposition of $CaCO_3$ is also observed between 618.9°C to 766.0°C which results in 8.60% of weight loss. Using the Eqn. 3, the weight percentage of $CaCO_3$ in this sample is calculated to be 19.56%. This verifies the higher formation of $CaCO_3$ with longer CO_2 curing duration.

In cementitious materials such as the artificial aggregates, $Ca(OH)_2$ and $CaCO_3$ plays a crucial role in the curing process of aggregates. $Ca(OH)_2$ is produced as a byproduct of cement hydration. Because it participates in the synthesis of important hydration products like calcium silicate hydrate (C–S–H), this molecule is essential to the

Int. Journal of Integrated Engineering Vol. 17 No. 1 (2025) p. 176-189

curing process. C–S–H has a major role in the durability and strength of aggregates [30]. Throughout the curing time, $Ca(OH)_2$ is gradually released, supporting the ongoing synthesis of C–S–H and aiding in the densification and reinforcing of the concrete matrix. Furthermore, while it may have an impact on alkalinity, the carbonation of $Ca(OH)_2$ to generate $CaCO_3$ can improve the durability of concrete by decreasing permeability and raising material density [31].

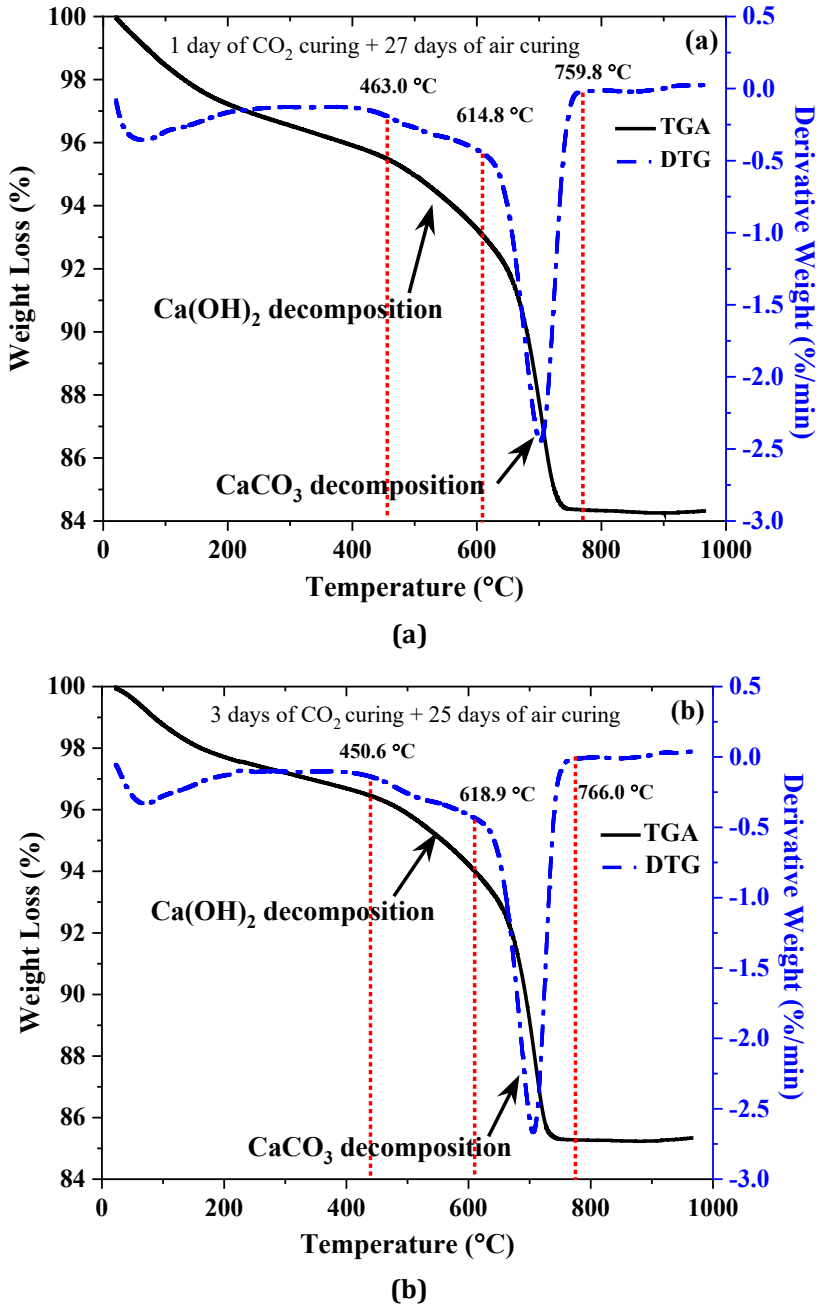

Fig. 10 *TGA/DTG curves of artificial aggregate (a) 1 day of CO_2 curing followed by 27 days of air curing; (b) 3 days of day of CO_2 curing followed by 25 days of air curing*

4. Conclusions

This study investigated the influence of CO_2-air and CO_2-water curing regimes on the mechanical and CO_2-capturing properties of artificial aggregates. The individual crushing strength of the aggregates was compared based on size, revealing that aggregates in the 5–6 mm range showed the highest value. Additionally, the ACV comparison of selected artificial aggregates showed that artificial aggregates subjected to CO_2-air curing consistently demonstrated lower ACV as compared to artificial aggregate that underwent CO_2-water curing, confirming higher strength. The phenolphthalein test revealed that artificial aggregates subjected to CO_2-air curing exhibited full carbonation, while artificial aggregates subjected to CO_2-water curing exhibited lower

carbonation as indicated by the changing of aggregates' colour from grey to pink when phenolphthalein solution was sprayed. The TGA/DTG curve of artificial aggregates with 1 and 3 days of CO_2-air curing demonstrated that a longer CO_2 curing duration resulted in greater $CaCO_3$ formation, as evidenced by the larger area under the curve in the $CaCO_3$ decomposition range. The TGA/DTG results supported the findings from the individual crushing strength and ACV tests, indicating that extended CO_2 curing improved the mechanical properties of the artificial aggregates. Overall, these findings suggest that integrating CO_2-air curing process significantly enhances the mechanical and CO_2 capturing properties of cement-slag artificial aggregates. The current work may contribute to a better understanding of sustainable building materials and their potential applications.

Acknowledgement

The authors would like to thank the Faculty of Civil Engineering, Universiti Teknologi Malaysia for supporting the research. This work was also supported by PETRONAS Research Sdn. Bhd. under Grant No. R.J130000.7622.4C806. The financial support provided by PETRONAS Research Sdn. Bhd. was essential for the successful completion of this project. We also gratefully acknowledge the in–kind support from Pan–United Concrete Pte. Ltd. for providing the raw material of Ground Granulated Blast Furnace Slag (GGBS).

Conflict of Interest

Authors declare that there is no conflict of interests regarding the publication of the paper.

Author Contribution

The authors confirm contribution to the paper as follows: ***study conception and design:*** *Abila Hena Anayet, Nur Hafizah A. Khalid;* ***data collection:*** *Abila Hena Anayet, Md Sajid Alam;* ***analysis and interpretation of results:*** *Abila Hena Anayet, Nurdalina Syuhada Zulkifli, Nur Hafizah A. Khalid, Mohamad Haqzim Ayob, Siti Aishah Jupri;* ***draft manuscript preparation:*** *Abila Hena Anayet, Mohamad Haqzim Ayob, Siti Aishah Jupri;* ***proofread:*** *Nor Hafizah Berahim, Hazratul Mumtaz Lahuri, Farahdila Kadirkhan. All authors reviewed the results and approved the final version of the manuscript.*

References

[1] Izumi, Y., Iizuka, A., & Ho, H-J. (2021) Calculation of greenhouse gas emissions for a carbon recycling system using mineral carbon capture and utilization technology in the cement industry, *Journal of Cleaner Production*, *312*, 127618, https://doi.org/10.1016/j.jclepro.2021.127618

[2] Xu, M., Zhao, Q., Mo, L., & Chen, B. (2024). Preparation of carbon-negative artificial lightweight aggregates by carbonating sintered red mud (SRM): CO_2 sequestration, microstructure and performance. *Journal of Cleaner Production, 469*, 143207. https://doi.org/10.1016/j.jclepro.2024.143207

[3] Mehdizadeh, H., Meng, Y., Guo, M. Z., & Ling, T. C. (2021). Roles of CO_2 curing induced calcium carbonates on high temperature properties of dry-mixed cement paste. *Construction and Building Materials, 289*, 123193. https://doi.org/10.1016/j.conbuildmat.2021.123193

[4] Lu, B., He, P., Liu, J., Peng, Z., Song, B., & Hu, X. (2021). Microstructure of Portland cement paste subjected to different CO_2 concentrations and further water curing. *Journal of CO_2 Utilization, 53(July),* 101714. https://doi.org/10.1016/j.jcou.2021.101714

[5] Lyu, J., Zhao, S., Xing, C., Wang, C., Chu, G., Xi, X., Zhou, C., Song, L., Ma, K., & Yue, H. (2024). The production of artificial aggregates with flue gas desulfurization ash: Development of a novel carbonation route. *Journal of Cleaner Production, 444*. https://doi.org/10.1016/j.jclepro.2024.141068

[6] Ahmed, O., Ahmad, S., & Adekunle, S. K. (2024). Carbon dioxide sequestration in cementitious materials: A review of techniques, material performance, and environmental impact. *Journal of CO_2 Utilization, 83*. https://doi.org/10.1016/j.jcou.2024.102812

[7] Khankhaje, E., Kim, T., Jang, H., Kim, C. S., Kim, J., & Rafieizonooz, M. (2024). A review of utilization of industrial waste materials as cement replacement in pervious concrete: An alternative approach to sustainable pervious concrete production. *Heliyon, 10 (4).* e26188. https://doi.org/10.1016/j.heliyon.2024.e26188

[8] Umar Khan M., Nasir M., Baghabra Al–Amoudi O. S., and Maslehuddin M., (2021) Influence of in–situ casting temperature and curing regime on the properties of blended cement concretes under hot climatic conditions, *Construction Building Materials*, 272, 121865. https://doi.org/10.1016/j.conbuildmat.2020.121865

[9] Wu, H., He, M., Wu, S., Cheng, J., Wang, T., Che, Y., Du, Y., & Deng, Q. (2024). Effects of binder component and curing regime on compressive strength, capillary water absorption, shrinkage and pore structure of geopolymer mortars. *Construction and Building Materials, 442*, 137707. https://doi.org/10.1016/j.conbuildmat.2024.137707

[10] Lee J. M., Yang H. J., Jang I. Y., Kim S. K., and Jung D. H., (2022) Comparison of calcium aluminate cements on hydration and strength development at different initial curing regimes, *Case Studies in Construction Materials*, 17, e01596, https://doi.org/10.1016/j.cscm.2022.e01596
[11] Galusnyak S. C., Petrescu L., and Cormos C. C., (2022), Environmental impact assessment of post–combustion CO_2 capture technologies applied to cement production plants, *Journal of Environmental Management,* 320, 115908, https://doi.org/10.1016/j.jenvman.2022.115908
[12] Zhang S., Ghouleh Z., Mucci A., Bahn O., Provençal R., and Shao Y., (2022), Production of cleaner high–strength cementing material using steel slag under elevated–temperature carbonation, *Journal of Cleaner Production*, 342, 130948, https://doi.org/10.1016/j.jclepro.2022.130948
[13] Liu, M., Hong, S., Wang, Y., Zhang, J., Hou, D., & Dong, B. (2021). Compositions and microstructures of hardened cement paste with carbonation curing and further water curing. *Construction and Building Materials, 267*, 121724. https://doi.org/10.1016/j.conbuildmat.2020.121724
[14] Liu, H., & Li, Q. (2023). Preparation of artificial aggregates from concrete slurry waste and waste brick masonry powder: CO_2 uptake and performance evaluation. *Construction and Building Materials, 382*. https://doi.org/10.1016/j.conbuildmat.2023.131356
[15] Shangwei Wang, Bo Wang, Haitang Zhu, Gang Chen, Zongze Li, Lin Yang, Yakun Zhang, Xiangming Zhou, (2023), Ultra–high performance concrete: Mix design, raw materials and curing regimes–A review," *Materials Today Communications, 35*, 105468, https://doi.org/10.1016/j.mtcomm.2023.105468.
[16] Jiang Y., and Ling T. C., (2020) Production of artificial aggregates from steel–making slag: Influences of accelerated carbonation during granulation and/or post–curing, *Journal of CO2 Utilization, 36*, 135–144, https://doi.org/10.1016/j.jcou.2019.11.009.
[17] Ashraf W., (2016) Carbonation of cement–based materials: Challenges and opportunities, *Construction and Building Materials*, 120, 558–570. https://doi.org/10.1016/j.conbuildmat.2016.05.080
[18] Kazemian M., and Shafei B., (2023), Carbon sequestration and storage in concrete: A state–of–the–art review of compositions, methods, and developments, *Journal of CO_2 Utilization*, 70, 102443, https://doi.org/10.1016/j.jcou.2023.102443
[19] Liu B., Qin J., Shi J., Jiang J., Wu X., and He Z., (2021), New perspectives on utilization of CO_2 sequestration technologies in cement–based materials, *Construction and Building Materials, 272*, 121660, https://doi.org/10.1016/j.conbuildmat.2020.121660
[20] Mo L., Yang S., Huang B., Xu L., Feng S., and Deng M., (2020) Preparation, microstructure and property of carbonated artificial steel slag aggregates used in concrete, *Cement and Concrete Composites, 113*, 103715, https://doi.org/10.1016/j.cemconcomp.2020.103715
[21] Sharma R., Pei J., and Jang J. G., (2023), Microstructural evolution of belite–rich cement mortar subjected to water, carbonation, and hybrid curing regime, *Cement and Concrete Composites, 139*, 105028, https://doi.org/10.1016/j.cemconcomp.2023.105028
[22] Yu Chen K., Jin Xia, Ren–jie Wu, Xin–yuan Shen, Jie–jing Chen, Yu–xi Chao, Wei–liang Jin, (2022) An overview on the influence of various parameters on the fabrication and engineering properties of CO_2–cured cement–based composites, *Journal of Cleaner Production, 366*, 132968, https://doi.org/10.1016/j.jclepro.2022.132968
[23] Shi C. and Wu Y., (2008) Studies on some factors affecting CO_2 curing of lightweight concrete products, Resources, *Conservation and Recycling, 52 (8–9),* 1087–1092, https://doi.org/10.1016/j.resconrec.2008.05.002
[24] Pang B., Zhou Z., and Xu H., (2015) Utilization of carbonated and granulated steel slag aggregates in concrete, *Construction and Building Materials, 84*, 454–467, https://doi.org/10.1016/j.conbuildmat.2015.03.008
[25] Ibrahim, M. A., Atmaca, N., & Atmaca, A. (2023), Physical and Mechanical Properties of an Artificial Aggregates Made up of Ground Granulated Blast–Furnace Slag. *Cihan University–Erbil Scientific Journal, 7 (2),* 26–30 . http://dx.doi.org/10.24086/cuesj.v7n2y2023.pp26–30
[26] Jiang Y. and Ling T. C., (2020), Production of artificial aggregates from steel–making slag: Influences of accelerated carbonation during granulation and/or post–curing, *Journal of CO_2 Utilization, 36*, 135–144, https://doi.org/10.1016/j.jcou.2019.11.009
[27] Gesoğlu M., Güneyisi E., and Öz H. Ö., (2012), Properties of lightweight aggregates produced with cold–bonding pelletization of fly ash and ground granulated blast furnace slag, *Materials and Structure, 45 (10)* 1535–1546, https://doi.org/10.1617/s11527–012–9855–9
[28] Jiang Y., Peng L., Ma Z., J. xin Lu, P. Shen, and C. S. Poon, (2023) Enhancing the treatment efficiency of recycled concrete fines with aqueous carbonation, *Cement and Concrete Research, 174*, 107338, https://doi.org/10.1016/j.cemconres.2023.107338

[29] Chu D. C., Kleib J., Amar M., Benzerzour M., and Abriak N. E., (2021) Determination of the degree of hydration of Portland cement using three different approaches: Scanning electron microscopy (SEM–BSE) and Thermogravimetric analysis (TGA), *Case Studies in Construction Materials, 15*, e00754, https://doi.org/10.1016/j.cscm.2021.e00754
[30] Neville, A.M. (2011) *Properties of Concrete*. Pearson Education Limited, Essex.
[31] Latawiec R., Woyciechowski P., and Kowalski K. J., (2018) Sustainable Concrete Performance—CO_2–Emission, *Environments, 5 (2)*, 1–14, https://doi.org/10.3390/environments5020027